

UNIVERSIDADE ESTADUAL DE CAMPINAS
SISTEMA DE BIBLIOTECAS DA UNICAMP
REPOSITÓRIO DA PRODUÇÃO CIENTÍFICA E INTELECTUAL DA UNICAMP

Versão do arquivo anexado / Version of attached file:

Versão do Editor / Published Version

Mais informações no site da editora / Further information on publisher's website:

<https://aip.scitation.org/doi/10.1063/1.4913625>

DOI: 10.1063/1.4913625

Direitos autorais / Publisher's copyright statement:

©2015 by AIP Publishing. All rights reserved.

DIRETORIA DE TRATAMENTO DA INFORMAÇÃO

Cidade Universitária Zeferino Vaz Barão Geraldo

CEP 13083-970 – Campinas SP

Fone: (19) 3521-6493

<http://www.repositorio.unicamp.br>

Surface effects on the mechanical elongation of AuCu nanowires: De-alloying and the formation of mixed suspended atomic chains

M. J. Lajos,^{1,2,a)} P. A. S. Autreto,¹ J. Bettini,² F. Sato,³ S. O. Dantas,³ D. S. Galvao,^{1,b)} and D. Ugarte¹

¹*Instituto de Física Gleb Wataghin, Universidade Estadual de Campinas, R. Sérgio B. de Holanda 777, 13083-859 Campinas-SP, Brazil*

²*Laboratório Nacional de Nanotecnologia-LNNANO, 13083-970 Campinas-SP, Brazil*

³*Departamento de Física, ICE, Universidade Federal de Juiz de Fora, 36036-330 Juiz de Fora-MG, Brazil*

(Received 2 December 2014; accepted 14 February 2015; published online 2 March 2015)

We report here an atomistic study of the mechanical deformation of $\text{Au}_x\text{Cu}_{(1-x)}$ atomic-size wires (nanowires (NWs)) by means of high resolution transmission electron microscopy experiments. Molecular dynamics simulations were also carried out in order to obtain deeper insights on the dynamical properties of stretched NWs. The mechanical properties are significantly dependent on the chemical composition that evolves in time at the junction; some structures exhibit a remarkable de-alloying behavior. Also, our results represent the first experimental realization of mixed linear atomic chains (LACs) among transition and noble metals; in particular, surface energies induce chemical gradients on NW surfaces that can be exploited to control the relative LAC compositions (different number of gold and copper atoms). The implications of these results for nanocatalysis and spin transport of one-atom-thick metal wires are addressed. © 2015 AIP Publishing LLC.

[<http://dx.doi.org/10.1063/1.4913625>]

I. INTRODUCTION

Predicting the mechanical behavior of a strained nanoscale volume of matter is essential for many nanotechnological applications.¹ This has stimulated an intense study of mechanical elongation of atomic-size metal nanowires (NWs).² In this range size ($\sim 1\text{--}2\text{ nm}$ in diameter), surface energy plays a dominant role, and factors that are neglected in macroscopic theory, such as size and shape, determine deformation mechanisms. For example, surface energy can induce strengthening and asymmetrical mechanical response.^{3–6} In addition, the high surface/volume ratio (SVR) may lead to the generation of anomalous helicoidal or tubular nanostructures during deformation.^{7,8}

Alloying or doping is routinely utilized to improve the mechanical resistance of metals (solute strengthening).⁹ However, these manipulations are very difficult to apply to nanosystems due to the huge SVR, which may promote composition gradients or even the expelling of impurities.^{10–12} In addition, most of our knowledge on metal alloy nanosystem is associated with heterogeneous catalysts, where the use of alloy nanoparticles (NPs) represents an active research field. Nanoscale mechanical deformation of alloys represents a quite complex topic, as the constant injection of elastic energy into the system may be relaxed through a wide variety of structural, physical, and chemical mechanisms. We also must keep in mind that the analysis of compositional gradients and segregation in alloy metal nanoparticles in heterogeneous catalysis still represent a question that awaits for

a reliable answer. A recent cutting edge study reports the analyses of composition gradients in metal nanoparticles exploiting X ray TEM tomography.¹³ In this way, this research remains quite challenging, as we must analyze the complex interplay between elastic, electronic, and surface energy contributions.

Here, we present a detailed study of atomic structure evolution of Au-Cu alloy NWs following tensile deformation by means of high resolution transmission electron microscopy (HRTEM). Molecular dynamics simulations were also carried out in order to analyze the dynamics of atomistic processes involved in the nanoalloy physical and chemical modifications.

II. METHODOLOGY

We have generated metal NWs from alloy bimetallic films ($\text{Au}_x\text{Cu}_{(1-x)}$ ($0 < x < 1$)) following the experimental procedure introduced by Takayanagi's group.¹⁴ Initially, holes are opened at several points in a self-supported metal film by focusing the microscope electron beam (300 A/cm^2); in this manner, nanometric constrictions (bridges) are formed between them. Then, the microscope beam current density is reduced to standard operation values (1030 A/cm^2) for image acquisition; in this range of beam current density, the HRTEM sample temperature is estimated to be within $300\text{--}350\text{ K}$.¹⁵ The spontaneous elongation and rupture of the nanowires are acquired using a high-sensitive TV camera (Gatan 622SC, 30 frames/s) and a standard video/DVD recorder. It is important to emphasize that this experimental procedure allows the acquisition of time-resolved atomic-resolution-imaging of NWs with a remarkable quality; nevertheless, it is not possible neither to measure the force being applied nor to control the stretching direction.¹⁶

^{a)}Present Address: Institute for Advanced Materials, Devices and Nanotechnology - IAMND, Rutgers University, Piscataway, New Jersey 00854, USA

^{b)}galvao@ifi.unicamp.br

Usually, the NW stretching and fracture occur with average displacement rates of 0.1–1 nm/s. The work described here used bimetallic Au_xCu_{1-x} alloy thin films as initial sample to generate NWs *in situ* in the HRTEM (JEM-3010 URP 300 kV, 0.17 nm point resolution).

Polycrystalline Au_xCu_{1-x} films (30–50 nm in thickness) have been prepared by thermal co-evaporation in a standard vacuum evaporator (10^{-7} mbar). A quartz crystal monitor was used to set the evaporation rate of each individual metal source and subsequently to measure the equivalent thickness of the film. Owing to higher cooling rates associated with the film deposition, the bimetallic films are expected to consist of a solid solution with random distribution of gold and copper atoms,¹⁷ what was confirmed by micro-electron diffraction results. To prevent possible oxidation by exposure to ambient conditions, the bi-metallic films were sandwiched between two (3-nm-thick) amorphous carbon thin layers. Before generating the NWs, the carbon layers are removed by strong electron irradiation¹⁸ inside the HRTEM. The structural characterization has been performed by means of micro-electron diffraction (JEM 2100 ARP, operated at 200 kV). In our experiments, the electron diffraction patterns (DP) were acquired from a region of 800 nm in diameter and recorded using a CCD camera (Gatan ES500W) (for more details see Figure S1 in the supplementary material (SM)³³). We have also measured the chemical composition of synthesized alloy films using Energy-Dispersive X-ray Spectroscopy (EDS); the Au_xCu_{1-x} alloy films were supported over conventional molybdenum TEM grids to avoid spurious x-ray signal. In particular, we analyzed several localized regions inside the initial illuminated area used for electron diffraction studies, and the observed atomic composition variations were within the typical composition error bar (5%, using Cliff-Lorimer method without absorption correction¹⁵). Also, the measured compositions were in very good agreement with electron diffraction estimation using Vegard's law. However, we have observed significant composition changes when comparing measurements performed in pristine alloy thin films and after the *in-situ* formation of NWs (i.e., after intense electron beam irradiation during several hours). It is important to highlight that the electron irradiation necessary to prepare the metal alloy film for a NW study requires several hours long electron beam irradiation. In contrast, the final NW elongation and rupture processes recorded by the experimental videos last, at most, 3–5 min at a much lower electron beam intensity (see description of electron microscopy works in Sec. I A of supplementary material³³); then, it is reasonable to think that no significant chemical composition change occurs during the nanowires imaging study. In this sense, we have assumed that the final EDS estimated concentration is a good value to describe the NW composition, and it has been used to describe the nanowires.

We have also carried out molecular dynamics simulations to gather deeper insights on the atomistic processes occurring during the alloy NW elongation. A tight-binding molecular dynamics methodology based on the second-moment approximation (TB-SMA)^{19,20} was used to analyze the elongation structural evolution. The theoretical methodology has already

been described in detail by Sato *et al.*,²¹ this approach has proved to be very effective for the study of Au and Cu NWs.^{18,22,23}

III. RESULTS

The *in-situ* HRTEM experiments indicate that $Au_xCu_{(1-x)}$ alloy NWs can deform along only three [111], [100], and [110] crystallographic directions. NWs elongated along [111] and [100] directions generate by-pyramidal constrictions that always evolve into an atomic contact or linear atomic chains (LACs); this behavior is identical to pure Au or Cu wires.^{3,23} In contrast, alloy NWs stretched along the [110] direction (hereafter noted as [110] NWs) display a concentration dependent structural behavior. While [110] Au NWs display rod-like morphology and break abruptly when formed by 3–4 atomic layer thick,^{3,22} alloy NWs (both $Au_{0.55}Cu_{0.45}$ and $Au_{0.2}Cu_{0.8}$) display a structural sequence typical of pure Cu wires:^{18,23} (1) rod-like wire; (2) by-pyramidal constrictions, and (3) a final one-atom-thick contact or LAC formation (Figures 1(b), 1(c), and corresponding videos in the SM). This indicates that a Cu content of $\sim 45\%$ is enough to trigger typical copper behavior, consequently modifying the rupture mode from brittle to ductile. These results are quite different from the $Au_xAg_{(1-x)}$ NW case,

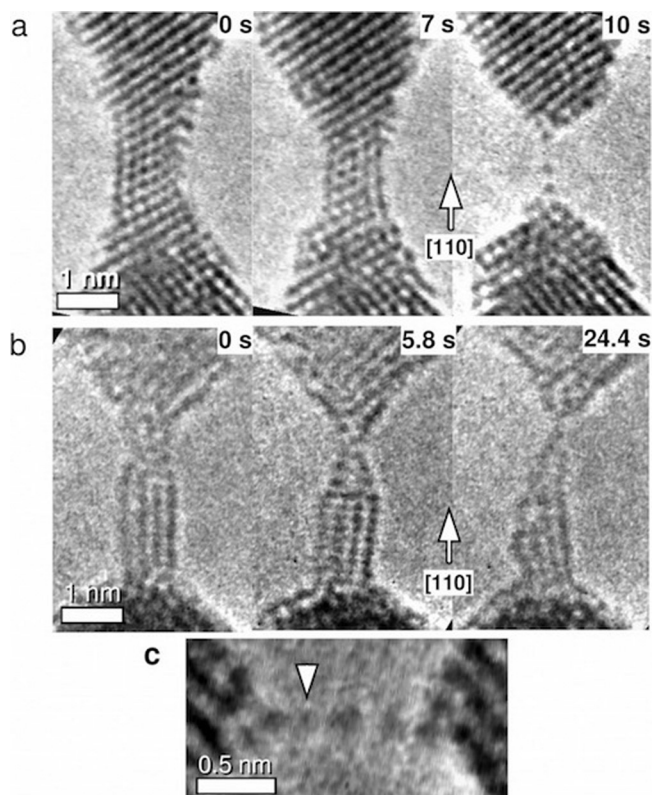


FIG. 1. Sequence of atomic resolution images associated with the elongation and thinning of rod-like [110] Au-Cu NWs as a function of chemical composition (atom positions appear dark). (a) $Au_{0.55}Cu_{0.45}$ and (b) $Au_{0.2}Cu_{0.8}$ NWs form by-pyramidal constrictions and evolve into either suspended atomic chains or atomic contact. (c) Closer view of suspended linear atomic chain generated from a $Au_{0.55}Cu_{0.45}$ NW; we can see that the atom at the left of the LAC (arrowed) displays a different contrast from the other suspended atoms suggesting the formation of mixed Au-Cu chains.

where a much higher Ag content ($\sim 80\%$) was necessary to reveal silver nanowire characteristics.¹¹

From a mechanical point of view, it is important to analyze the active deformation mechanisms of atomic-size alloy wires. Concerning bulk material, Au and Cu are Face Centered Cubic (FCC) metals and plastic deformation occurs mostly by the gliding of compact (111) atomic planes along [112]-type directions. In particular, partial edge dislocations (PDs) are formed, which encapsulate a stacking fault (SF) ribbon. In tiny gold nanorods, where diameter (~ 1 nm) is smaller than the SF ribbon width ($(d) \sim 2\text{--}3$ nm in bulk⁹), plastic deformation occurs by the formation of planar defects that generates a compact glide (block on a block) of the (111) planes by $(1/6)[112]$.^{5,24} In these very tiny wires, thermal energy at room temperature is enough to recombine these planar faults^{5,25} and pure Au and pure Cu NWs stay defect free when stretched at 300 K.^{3,23,26,27} Concerning macroscopic alloys, it is well known that alloying influences drastically the elastic modulus and yield strength.⁹ On this basis, we could expect that in Au-Cu alloy NWs, energy barrier blocking planar defects should be higher. In fact, we have observed the formation of planar defects at room temperature in some NWs with $\text{Au}_{0.55}\text{Cu}_{0.45}$ composition (Figures 2(a) and 2(b)). Nevertheless, many alloy NWs also displayed defect free structures; this may be associated with subtle local variations of chemical composition inside the alloy thin film or be even induced during the wire elongation.¹¹ Figures 2(c) and 2(d) show some interesting images of $\text{Au}_{0.20}\text{Cu}_{0.80}$ NWs. Note several darker dots at the NW apexes. This might be associated with the formation of several small gold clusters during the NW elongation (gold atoms are expected to generate darker dots in the images). Accordingly, our video recordings show that these clusters move slowly during the mechanical elongation, suggesting that they may be located on the NW surface (see SM

(Ref. 33)). In fact, several theoretical studies of Au-Cu nanoparticles have predicted the migration of gold atoms to the surface in order minimize surface energy.^{10,28} Certainly, the gold lower surface energy²⁹ and lower diffusion barrier drive gold atoms migration to the wire surface during the mechanical deformation.

Molecular dynamics simulations can provide additional insight into atom reorganization and redistribution during alloy NW elongation. Figure 3(a) shows a sequence of snapshots of the stretching of $\text{Au}_{0.5}\text{Cu}_{0.5}$ NW along [110] direction. Initially, a by-pyramidal constrictions is formed, in good agreement with experimental observations; then, a long NW is generated. It is important to emphasize that most of the NW gold atoms are located on the NW surface, the inset shows a cross-sectional view where it is clear that Au atoms enclose a chain of Cu atoms. Finally, a one-atom-thick contact is formed before breaking. During the elongation, a clear gold enrichment of the narrowest wire regions can be measured (see also data in the SM). Figure 3(b) shows a similar Au surface migration effect in $\text{Au}_{0.2}\text{Cu}_{0.8}$ NW stretched along [110] axis. However, the behavior changes, because the initial Au content is rather low (20%) and there are not enough available gold atoms to cover the whole surface.¹⁰ Finally, Figure 3(c) illustrates an $\text{Au}_{0.2}\text{Cu}_{0.8}$ NW being elongated along the [100] direction, which becomes gradually thinner until forming an atomic contact. The formation of small gold clusters (3–5 atoms) on the NW surface can be clearly observed. The segregated gold clusters remain coalesced and sometimes diffuse slowly on the NW surface. Briefly, the simulations have revealed two effects associated with local composition changes: (i) surface segregation of Au atoms and (ii) gold clustering. These effects are in excellent agreement with the experimental observations displayed in Figures 1 and 2. However, we must keep in mind that electron beam induced effects that may also influence atom diffusion or segregation. We think that these effects are negligible in our experiments due to the rather short duration of the experiments (less than 1 min for the elongation and rupture of the 1-nm-wide alloy wires, see a detailed discussion in the SM).

From a more fundamental point of view, the formation of one-atom-thick nanowires containing different metal atomic species, represents one of the most interesting nano-systems to study 1-D quantum physics. So far, mixed suspended LACs were experimentally produced only with gold and silver.¹¹ Mixed LACs containing gold and transition metal atoms open the possibility to address excellent physical and chemical questions, such as nanomagnetism, spin transport, s-d bonding in low dimensional systems, etc. From this perspective, the one-atom thick wire generated from the Au-Cu alloy nanowires observed in our study represents an excellent case study. Our HRTEM results indicate that suspended chains display variations in the intensity/contrast at atomic positions (see Figure 1(c) and SM), suggesting that they should be formed by both gold and copper atoms. A quantitative comparison between experimental and simulated HRTEM image intensities confirms this interpretation. The interatomic distances in the LAC are in the $[0.25\text{--}0.32]$ nm range, which agrees with impurity-free gold and copper

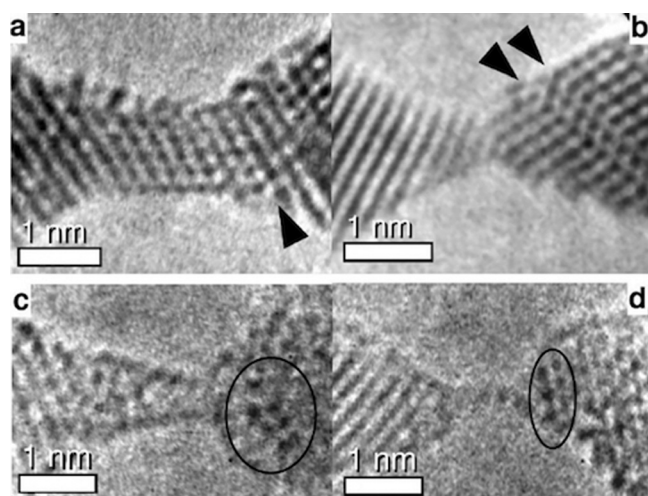


FIG. 2. Typical HRTEM images of $\text{Au}_{0.55}\text{Cu}_{0.45}$ NWs displaying planar defects (a) and twins (b). Defects are indicated by black arrows and they can also be identified by a discontinuity in the atomic planes. (c) and (d) HRTEM images of stretched $\text{Au}_{0.2}\text{Cu}_{0.8}$ NWs which indicate the formation of small gold clusters in the NW surface shown inside the ellipses. Atom positions appear dark.

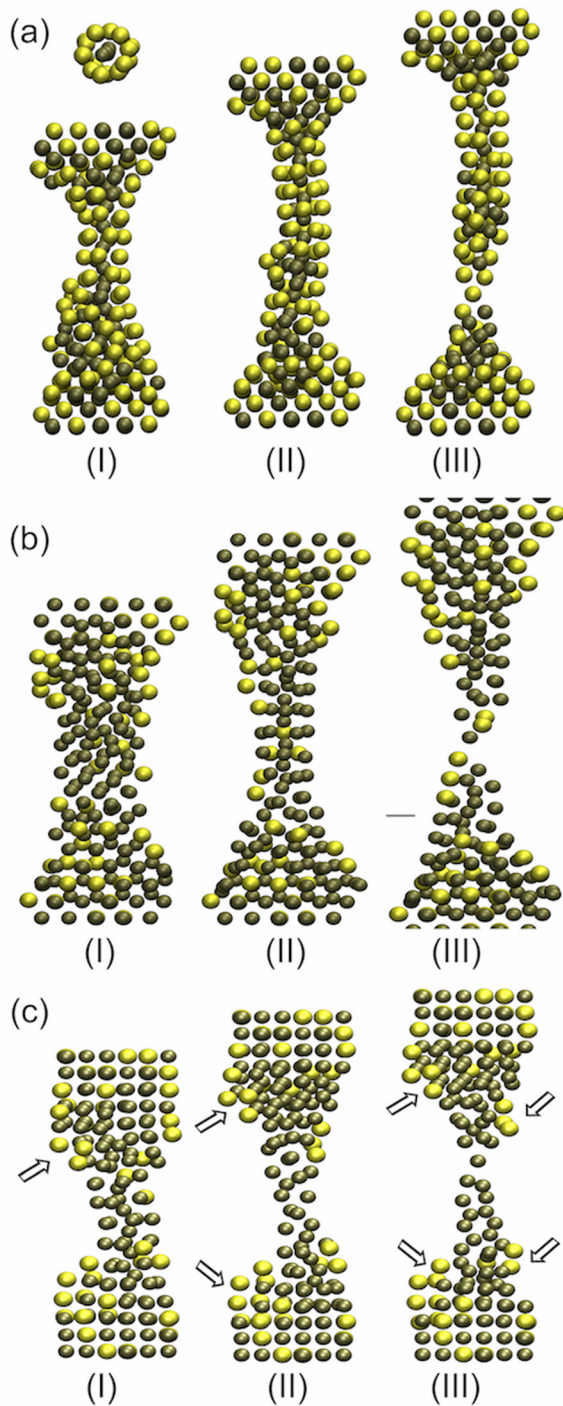


FIG. 3. Sequence of snapshots associated with the theoretical simulations of bi-metallic Au-Cu nanowire elongation. Gold and copper atoms are represented by yellow and dark gray balls, respectively. Figures (a) and (b) correspond to the elongation along [110] axis of $\text{Au}_{0.55}\text{Cu}_{0.45}$ and $\text{Au}_{0.2}\text{Cu}_{0.8}$ NWs, respectively. Note that in both cases, gold atoms have a tendency to occupy the NW surface. Figure (c) illustrates the formation of small gold clusters (3–5 atoms) on the NW surface (indicated by arrows) during the elongation of a $\text{Au}_{0.2}\text{Cu}_{0.8}$ NW along [100] axis. The corresponding animations can be found in the SM.

chains.^{23,30,31} Light possible impurity atoms, such as C, O, N should produce a much lower contrast than the signal noise ratio experimentally observed (see details in SM).

A natural question arises, can we control the LAC chemical composition by selecting the proper alloy, wire shape,

TABLE I. Statistical analysis of LAC formation from the molecular dynamics simulations. The three numbers (X/Y/Z) indicate the number of LAC formed and composed only of gold, mix Au/Cu or copper, respectively.

Au_xCu_y	[100]	[110]	[111]
50/50	6/3/0	6/4/0	2/6/2
80/20	2/2/7	4/3/2	3/7/1

elongation direction, etc.? Previous theoretical studies have shown that most of the atoms composing suspended chains come from the outermost layers for Au nanowires.²¹ With this idea in mind, we have analyzed our theoretical simulations and looked at the chemical composition (pure Au or Cu, or alloyed chains) of LACs generated along different stretching directions for different alloy compositions ($\text{Au}_{0.5}\text{Cu}_{0.5}$ and $\text{Au}_{0.2}\text{Cu}_{0.8}$). Most of suspended atomic chains were composed by two hanging atoms, while seldom rather long chains (4–5 atoms) were observed. Although, the rather low available statistics, a clear alloy composition and elongation direction dependence show up (see results in Table I). LACs generated from [100] NWs show the tendency to be either pure Au or pure Cu depending on the alloy mixture. In contrast, mixed LACs dominate the occurrence along [111] axis for both studied alloys. Finally, [110] alloy nanowires show a slight tendency to produce pure Au chains, followed by alloyed chains.

In order to understand these simulation results, we must first consider that alloy composition influences NW morphologies through changes in the surface energy of the different crystallographic facets.¹⁰ A gold particle should be a cuboctahedra with regular hexagonal facets (minimal energy planes are {111}),¹⁰ schema at left in Figure 4(a)), while Cu nanoparticle³² have a morphology dominated by {100} facets (center and right octahedra in Figure 4(a)). In first approximation, an alloy nanosystem behavior must be somewhat in between these two extrema.¹⁰ In addition, as diffusion and migration are enhanced in nanosystems, it is reasonable to make the hypothesis that the wires will have a spontaneous tendency to have composition gradient in the volume and on the surfaces. In particular, we can assume that {hkl} facets will accommodate more atoms of the chemical species that minimize the facets surface energy, which would lead to Au (Cu) rich {111} ({100}) facets in an Au-Cu alloy NW (or NP). A gold-rich-alloy NW along [100] should have a pyramidal shape of square base defined by four triangular {111} facets (see left side in Figure 4(b) (Ref. 3)). These facets will become Au rich during elongation, which finally will enhance the formation of pure Au LACs. In contrast, a Cu rich [100] NW should display a rod-like shape with a square cross section, the surface being formed by four {100} facets (see right side in Figure 4(b)), then having a tendency to generate mostly pure Cu LACS. Wires along [110] direction will have a hexagonal cross section formed by both {111} and {100} facets, with a relative weight that varies from Au to Cu; this explains why pure Au and mixed chains are formed along [110] elongation axis. Finally, alloy NWs formed along [111] will generate at some moment a triangular cross section (see, for example, the

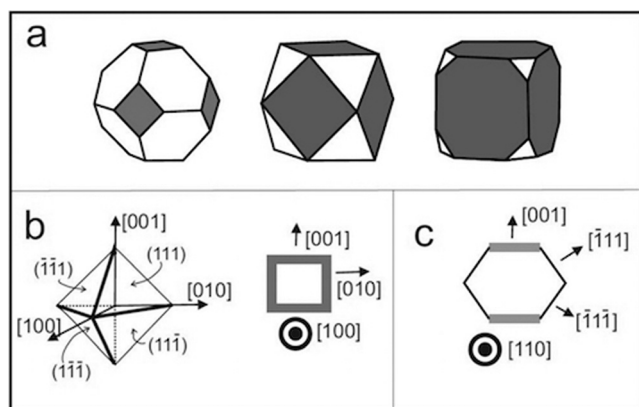


FIG. 4. (a) From left to right, shapes of cuboctahedral FCC nanoparticles increasing the relevance of $\{100\}$ facets in relation to $\{111\}$ facets. (b) Scheme of the possible $[100]$ alloy NW; a pyramidal shape containing only $\{111\}$ surfaces, expected for a gold rich wire and a rod-like wire of square cross-section expected for Cu rich NW (only $\{100\}$ facets cover the surface). (c) Qualitative hexagonal cross-section for a pillar-like wire expected along $[110]$ direction, note that this rod is formed by both $\{111\}$ and $\{100\}$ facets (see text for discussions).

$\{111\}$ facet shape of octahedra at the center of image 4(a)). This triangular facet is surrounded by three $\{100\}$ (Cu rich) facets and the tip of three $\{111\}$ (Au rich) facets, which can provide both Au and Cu atoms. This kind of wire must be expected to generate mostly mixed LACs, as in fact, we observed in the simulations.

In summary, we have observed that alloy $\text{Au}_x\text{Cu}_{(1-x)}$ NWs show a strong concentration dependence mechanical behavior. Approximately a $\sim 45\%$ Cu content is required to trigger copper-alike mechanical behavior. For the tiny alloy NWs studied here ($\sim \text{nm}$ in diameter), surface energy contribution is so important that can induce gold enrichment and even gold surface segregation during elongation. The formation of suspended atom chains containing Au and Cu atoms was experimentally revealed. Molecular dynamics simulations suggest that it is possible to control the LAC chemical composition by choosing the appropriate alloy composition and NW elongation direction. This would exploit the spontaneous formation of chemical composition gradients (or preferential chemical enrichment of each family of crystallographic facets) on the NW surface. This phenomena can certainly be expected to also happen in alloy nanoparticles and may modify significantly the reactivity and/or catalytic activity in heterogeneous catalysis. From another point of view, the possibility to generate, in a reasonable controlled way, alloy LACs containing Au and magnetic transition metals may open new opportunities for the study scattering and spin transport in one-atom-thick metal wires.

ACKNOWLEDGMENTS

P. C. Silva is acknowledged for assistance during HRTEM and sample preparation work. We acknowledge financial support from LNLS, FAPESP, and CNPq. The

authors thank the Center for Computational Engineering and Sciences at Unicamp for financial support through the FAPESP/CEPID Grant No. 2013/08293-7.

- ¹C. Alloca and D. Smith, "Instrumentation and metrology for nanotechnology," Report of the National Nanotechnology Initiative, see www.nano.gov, 2005, Chap. 3.
- ²G. Rubio, N. Agraït, and S. Vieira, *Phys. Rev. Lett.* **76**, 2302 (1996).
- ³V. Rodrigues, T. Führer, and D. Ugarte, *Phys. Rev. Lett.* **85**, 4124 (2000).
- ⁴S. Brinckmann, J.-Y. Kim, and J. R. Greer, *Phys. Rev. Lett.* **100**, 155502 (2008).
- ⁵M. J. Lagos, F. Sato, D. S. Galvão, and D. Ugarte, *Phys. Rev. Lett.* **106**, 055501 (2011).
- ⁶K. Sieradzki, A. Rinaldi, C. Friesen, and P. Peralta, *Acta Mater.* **54**, 4533 (2006).
- ⁷Y. Kondo and K. Takayanagi, *Science* **289**, 606 (2000).
- ⁸M. J. Lagos, J. Bettini, F. Sato, V. Rodrigues, D. S. Galvão, and D. Ugarte, *Nat. Nanotechnol.* **4**, 149 (2009).
- ⁹W. D. Callister, *Materials Science and Engineering: An Introduction* (John Wiley, New York, 2003).
- ¹⁰E. Ringe, R. P. Van Duyne, and L. D. Marks, *Nano Lett.* **11**, 3399 (2012).
- ¹¹J. Bettini, F. Sato, P. Z. Coura, S. O. Dantas, D. S. Galvão, and D. Ugarte, *Nat. Nanotechnol.* **1**, 182 (2006).
- ¹²S. C. Erwin, L. Zu, M. I. Haftel, A. L. Efros, T. A. Kennedy, and D. J. Norris, *Nature* **436**, 91 (2005).
- ¹³T. J. A. Slater, A. Macedo, S. L. M. Schroeder, M. Grace Burke, P. O'Brien, P. H. C. Camargo, and S. J. Haigh, *Nano Lett.* **14**, 1921 (2014).
- ¹⁴Y. Kondo and K. Takayanagi, *Phys. Rev. Lett.* **79**, 3455 (1997).
- ¹⁵C. B. Carter and D. B. Williams, *Transmission Electron Microscopy* (Springer, New York, 2009).
- ¹⁶V. Rodrigues and D. Ugarte, *Nanowires and Nanobelts*, edited by Z. L. Wang (Kluwer Academic Publishers, Boston, 2003), Vol. 1, Chap. 6.
- ¹⁷D. A. Porter and K. E. Easterling, *Phase Transformations in Metals and Alloys* (Chapman and Hall, London, 1992).
- ¹⁸F. Sato, A. S. Moreira, J. Bettini, P. Z. Coura, S. O. Dantas, D. Ugarte, and D. S. Galvão, *Phys. Rev. B* **74**, 193401 (2006).
- ¹⁹F. Cleri and V. Rosato, *Phys. Rev. B* **48**, 22 (1993).
- ²⁰D. Tománek, A. A. Aligia, and C. A. Balseiro, *Phys. Rev. B* **32**, 5051 (1985).
- ²¹F. Sato, A. S. Moreira, P. Z. Coura, S. O. Dantas, S. B. Legoas, D. Ugarte, and D. S. Galvão, *Appl. Phys. A* **81**, 1527 (2005).
- ²²P. Z. Coura, S. B. Legoas, A. S. Moreira, F. Sato, V. Rodrigues, S. O. Dantas, D. Ugarte, and D. S. Galvão, *Nano Lett.* **4**, 1187 (2004).
- ²³J. C. González, V. Rodrigues, J. Bettini, L. G. C. Rego, A. R. Rocha, P. Z. Coura, S. O. Dantas, F. Sato, D. S. Galvão, and D. Ugarte, *Phys. Rev. Lett.* **93**, 126103 (2004).
- ²⁴U. Landman, W. D. Luedtke, N. A. Burnham, and R. J. Colton, *Science* **248**, 454 (1990).
- ²⁵I. A. Ovid'ko and A. G. Sheinerman, *Rev. Adv. Mater. Sci.* **27**, 189 (2011), available online at http://www.ipme.ru/e-journals/RAMS/no_22711/ovidko.html.
- ²⁶J. R. Rice, *J. Mech. Phys. Solids* **40**, 239 (1992).
- ²⁷E. B. Tadmor and S. Hai, *J. Mech. Phys. Solids* **51**, 765 (2003).
- ²⁸J. L. Rodríguez-Lopez, J. M. Montejano-Carrizales, U. Pal, J. F. Sanchez-Ramirez, H. E. Troiani, D. Garcia, M. Miki-Yoshida, and M. Jose-Yacamán, *Phys. Rev. Lett.* **92**, 196102 (2004).
- ²⁹L. Vitos, A. V. Ruban, H. L. Skriver, and J. Kollar, *Surf. Sci.* **411**, 186 (1998).
- ³⁰M. J. Lagos, F. Sato, P. A. S. Autreto, D. S. Galvão, V. Rodrigues, and D. Ugarte, *Nanotechnology* **22**, 095705 (2011).
- ³¹S. B. Legoas, D. S. Galvão, V. Rodrigues, and D. Ugarte, *Phys. Rev. Lett.* **88**, 076105 (2002).
- ³²I. Lisiecki, A. Filankembo, H. Sack-Kongehl, K. Weiss, M. P. Pileni, and J. Urban, *Phys. Rev. B* **61**, 4968 (2000).
- ³³See supplementary material at <http://dx.doi.org/10.1063/1.4913625> for details of sample preparation, discussions of electron beam induced effects and HRTEM images analysis.